



Full length article

Static recrystallization and grain growth during annealing of an extruded Mg–Zn–Zr–Er magnesium alloy

Jing Zhang^{a,b,*}, Weiguo Li^a, Zhengxiao Guo^c

^a College of Materials Science and Engineering, Chongqing University, Chongqing 400044, China

^b National Engineering Research Center for Magnesium Alloys, Chongqing 400044, China

^c University College London, 20 Gordon Street, London WC1H 0AJ, UK

Abstract

Microstructure stability is essential to maintain a fine grain structure for an alloy throughout its processing. The effects of Er addition and its existing form on the static recrystallization and grain growth during annealing of an extruded Mg–1.5Zn–0.6Zr magnesium alloy were studied in this paper. The results showed that microstructure stability was much improved by Er addition and the best thermability was obtained in 2 wt.% Er-containing alloy. For the incomplete dynamic recrystallization (DRX) microstructures extruded at a lower temperature of 350 °C, Er addition increased the resistance of static recrystallization; and for the complete DRX microstructures extruded at a relatively high temperature of 420 °C, Er addition suppressed grain growth. The difference in microstructure stability was then correlated with the microstructure features. Both the intermetallic phase and the solute atoms of Er in α -Mg matrix contributed to the microstructure stability. Moreover, it is believed that the existing form of Er–Zn atom pairs in the α -Mg solid solution favored the most to improve the thermal stability of the alloy. Copyright 2013, National Engineering Research Center for Magnesium Alloys of China, Chongqing University. Production and hosting by Elsevier B.V. Open access under [CC BY-NC-ND license](https://creativecommons.org/licenses/by-nc-nd/4.0/).

Keywords: Magnesium alloy; Recrystallization; Grain growth; Rare earth element

1. Introduction

With a relatively high specific strength, magnesium alloys are desirable for many applications in microelectronics, aerospace and automobile industries. However, the wide application of magnesium alloy suffers heavily from its inferior absolute strength and poor ductility, compared with the present commonly used metal structural materials, such as

aluminum and steel. Due to the intrinsic nature of magnesium alloys, including hexagonal closepacked (hcp) lattice structure with a limited number of independent slip systems and no allotropic transformation along with temperature variation, the improvement of strength and ductility of magnesium has to depend on the combination of various strengthening mechanisms.

Grain size refinement is well known to be the only mechanism, among the four common strengthening mechanisms for metal materials, which can increase both strength and ductility. Strengthening via grain size control is particular effective to magnesium alloys because the Hall–Petch coefficient of magnesium alloys is notably higher than that for aluminum alloys and steel [1,2]. The stacking fault energy for magnesium was reported to be much smaller than aluminum and steel [3], dynamic recrystallization (DRX) thus readily occurs in magnesium alloys during hot working processes and has been shown to be a promising route for refining the microstructure [4,5]. However, commercial wrought magnesium alloys suffer

* Corresponding author. College of Materials Science and Engineering, Chongqing University, Chongqing 400044, China. Tel.: +86 23 65111167; fax: +86 23 65102821.

E-mail address: jingzhang@cqu.edu.cn (J. Zhang).

Peer review under responsibility of National Engineering Research Center for Magnesium Alloys of China, Chongqing University



from high tendency of grain growth at high temperature due to lack of effective solutions to stabilize the microstructures [6,7]. This will induce significant loss of strength and ductility during subsequent heat treatment or thermal mechanical processing of semi-products.

Rare earth (Re) elements have long been known for its beneficial effects on the elevated temperature properties of magnesium alloys. Re elements exist either in the form of solute atoms in Mg matrix or in the form of second-phase particles combining with the other alloying elements and/or Mg [8–14]. These phases normally have higher thermal stability and cannot be dissolved during conventional thermo-mechanical treatments. It is reported that these particles can be utilized to affect DRX and grain size [15]. However, how does Re affect the microstructure stability during subsequent heat treatment or thermal mechanical treatment and what the mechanism is remain unclear. Mg–Zn–Zr system alloys is an important commercial high strength wrought alloy. Previous

studies have shown Mg–Zn–Zr alloy with rare earth Er addition exhibits improved hot workability and DRX microstructures [16–18]. In this paper, the effects of Er addition and its existing form on the static recrystallization and grain growth during annealing of an extruded Mg–1.5Zn–0.6Zr magnesium alloy were studied. The results will be beneficial for an improved understanding of the fundamental mechanism necessary to develop new Mg alloys with stable and fine grain structures.

2. Experimental procedure

An Mg–1.5Zn–0.6Zr (wt.%) alloy has been chosen as a model alloy. The alloy was systematically added with 0, 0.5, 1, 2 and 4 wt.% Er. The alloys were prepared from commercial high-purity Mg (>99.9%) and Zn (>99.95%), and master alloys Mg–31wt.%Zr and Mg–30wt.%Er. All the materials added were melted in a steel crucible inside an electric

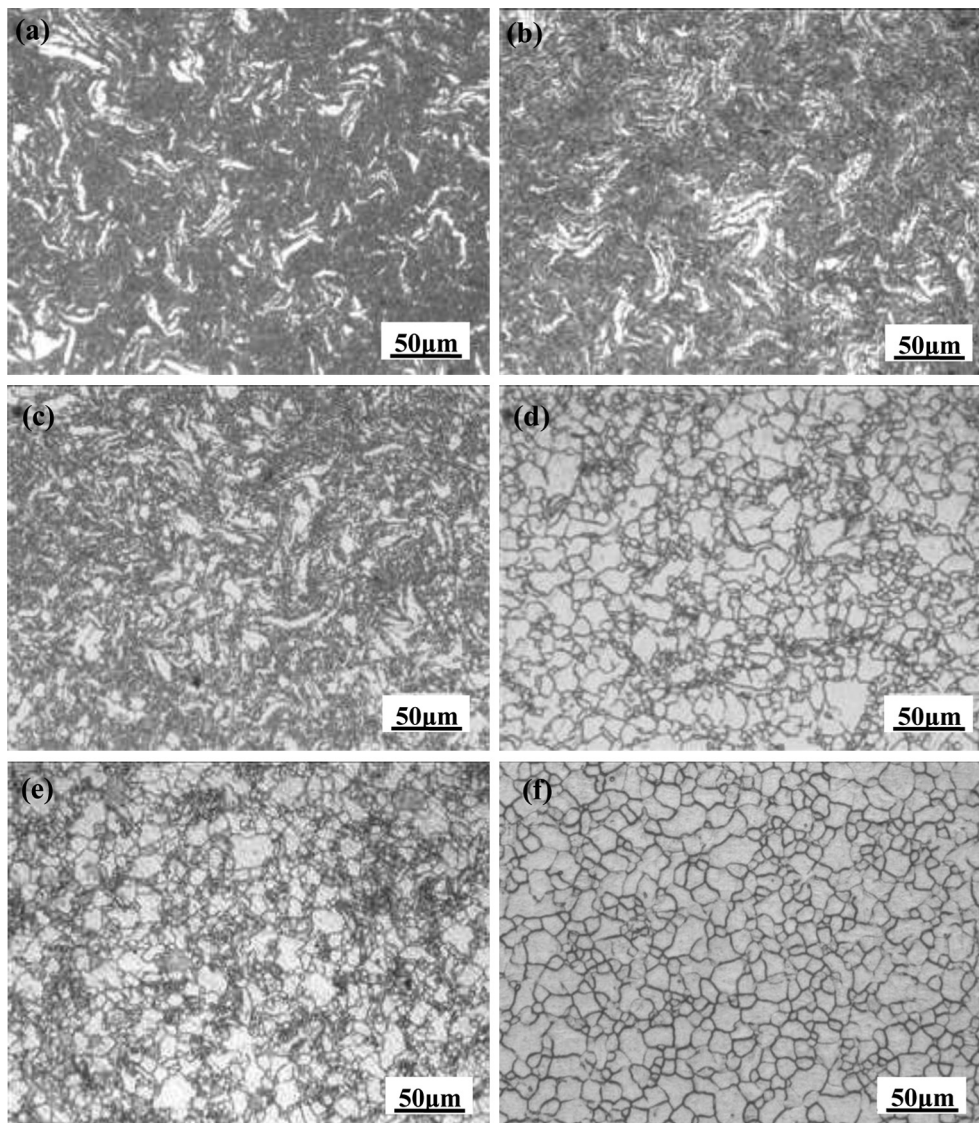


Fig. 1. Optical microstructures annealed at a) 250 °C, b) 300 °C, c) 315 °C, d) 335 °C, e) 350 °C and f) 400 °C for Mg–1.5Zn–0.6Zr alloy extruded at 350 °C.

resistance furnace. The molten metal was mechanically stirred during melting and held at 750 °C for 30 min. The melt was then cooled down to around 720 °C, and cast into ingots of 85 mm in diameter by semi-continuous casting under a ($\text{SO}_2 + \text{CO}_2$) protective gas mixture with water cooling. The ingots were then homogenized for 12 h at 410 °C and cooled in a furnace. After homogenization, the ingots were skinned and heated to the extrusion temperature for 1 h before extrusion. Two extrusion temperatures, 350 °C and 420 °C, were adopted, in order to obtain microstructures with a different DRX degree. Extrusion was conducted on a XJ-500 Horizontal Extrusion Machine. The extrusion ratio was 25. After extrusion, the alloys were cooled in the open air.

The extruded alloy bars were then annealed in the temperature range of 250–400 °C for a fixed time of 1.5 h. Samples sectioned from the annealed bars were polished and etched and then undergone microstructure observation by using Olympus optical microscope. Observation plane

was perpendicular to the extrusion axis. The grain size was measured by the mean liner intercept method.

3. Results and discussion

3.1. As-annealed microstructures for alloys extruded at 350 °C

The microstructures annealed at different temperatures in the range of 250–400 °C for Mg–1.5Zn–0.6Zr alloy extruded at 350 °C are shown in Fig. 1. Due to a heterogenous deformation behavior and the lower extrusion temperature, the alloy exhibited a non-uniform incomplete DRX microstructure with a large volume fraction of distorted original grains and an uneven grain distribution [18]. When annealed at a lower temperature of 250 °C, the volume fraction of the non-recrystallized original grains remains almost unchanged (white part), as shown in Fig. 1(a). Increasing the annealing

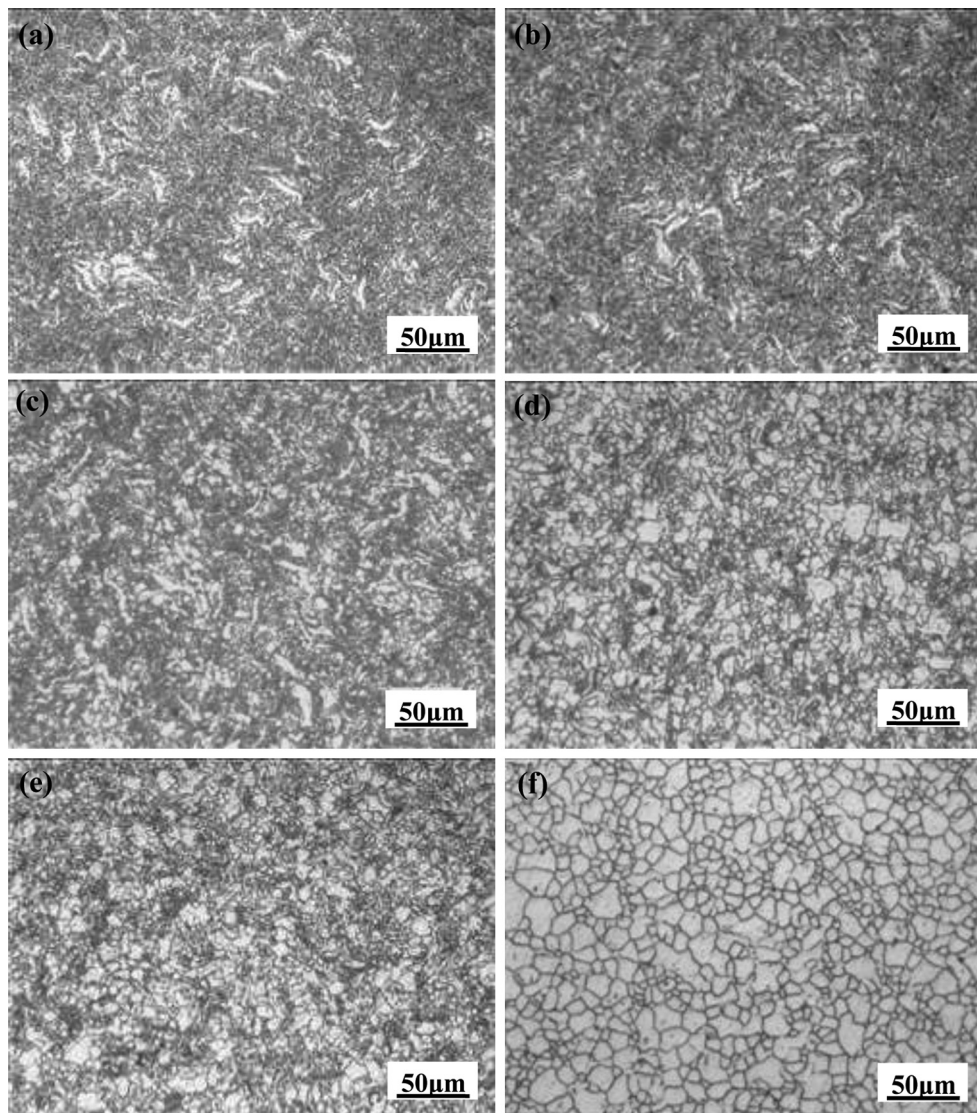


Fig. 2. Optical microstructures annealed at a) 250 °C, b) 300 °C, c) 315 °C, d) 335 °C, e) 350 °C and f) 400 °C for Mg–1.5Zn–0.6Zr–1Er alloy extruded at 350 °C.

temperature to 300 °C (Fig. 1(b)) and 315 °C (Fig. 1(c)) leads to a gradual decrease of the amount of the original grains, indicating a certain degree of static recrystallization occurred in this temperature range. When annealed at 335–350 °C (Fig. 1(d) and (e)), full static recrystallization occurred and the alloy manifests an equiaxed grain structure. However, the grain size still differs greatly and exhibits a typical mixed grain structure. Further increase of the annealing temperature results in grain growth and a homogenous grain distribution, shown in Fig. 1(f).

The microstructure evolution with annealing temperature for alloys with relatively low Er additions, i.e. 0.5–1%, shows a same tendency as the Er-free alloy. Static recrystallization began in the temperature range of 300–315 °C and a full static recrystallization occurred at around 335 °C. As an example, the microstructures at different annealing temperatures in the range of 250–400 °C for 1% Er-containing alloy are shown in

Fig. 2. With increasing Er addition, however, the alloy developed distinct microstructures along with annealing temperatures. As can be seen from Fig. 3, there is no noticeable change of the microstructures for the 2% Er-containing alloy even annealed at temperature as high as 350 °C. The distorted original grains diminished and full recrystallization occurred at around 365 °C, which is 30 °C higher than that for the alloys with lower or without Er addition.

For a clear comparison of the static recrystallization degree with annealing temperature for alloys with different Er additions, the variation of the area fraction of the distorted original grains with annealing temperature for different alloys was drawn in Fig. 4. It is noted that there is a sharp change point on each of the curves, followed immediately by a complete disappear of the deformed grains. This temperature range is reasonably thought to correspond to an obvious static recrystallization. As evidently shown in Fig. 4, the amount of the

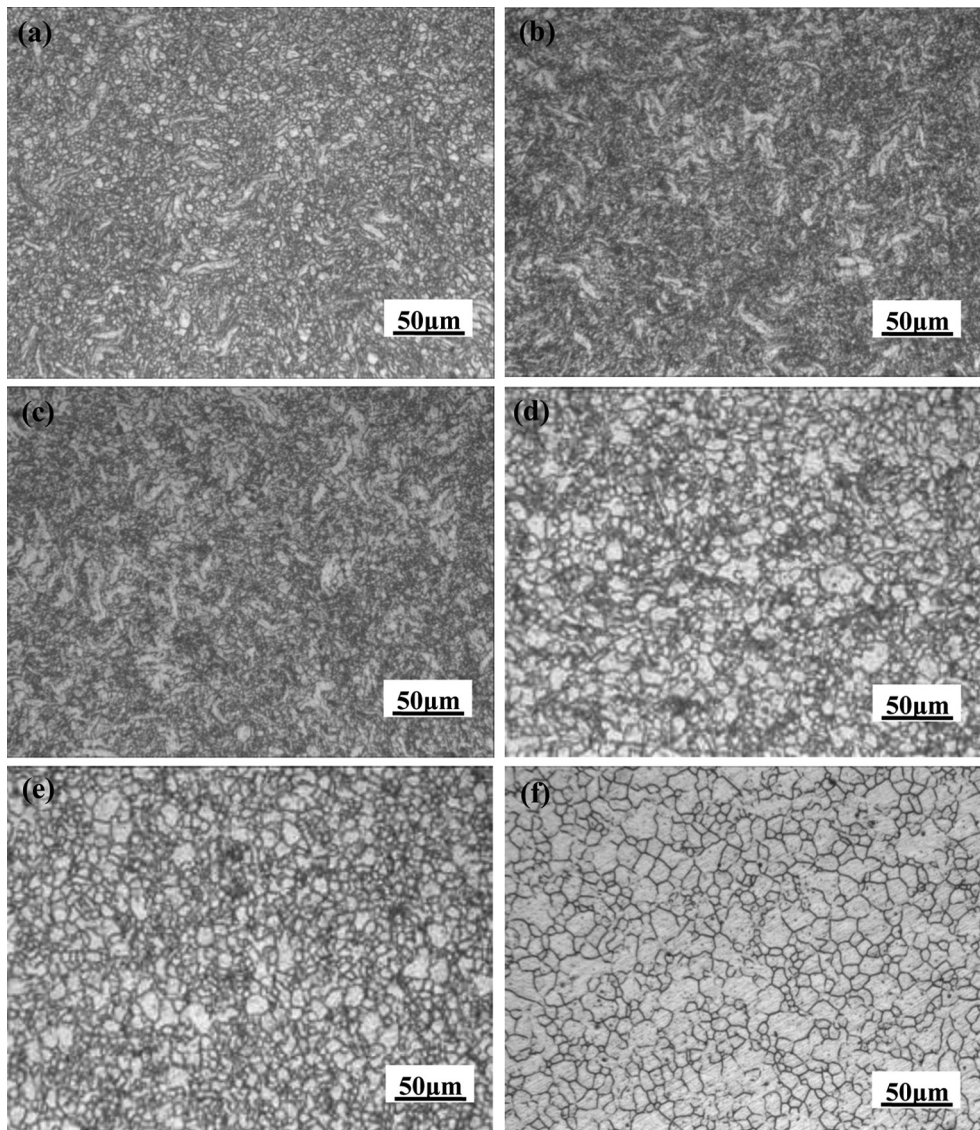


Fig. 3. Optical microstructures annealed at a) 250 °C, b) 300 °C, c) 350 °C, d) 365 °C, e) 380 °C and f) 400 °C for Mg–1.5Zn–0.6Zr–2Er alloy extruded at 350 °C.

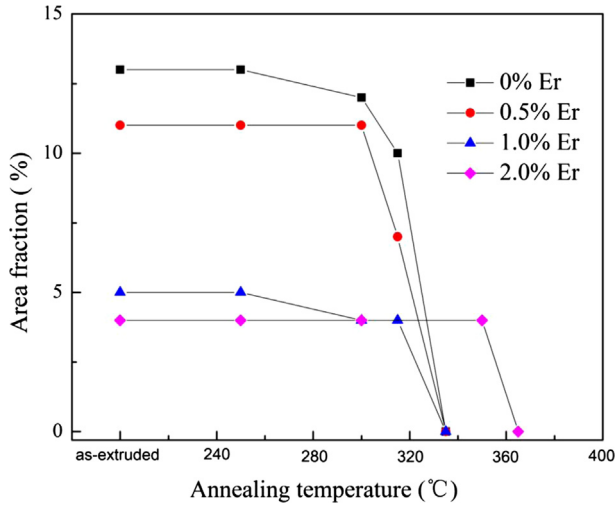


Fig. 4. Variation of the area fraction of non-recrystallized grains with annealing temperature for alloys with different Er addition.

original deformed grains decreases with the increase of Er addition, from ~13% in Er-free alloy to 11%, 5% and 4% in alloys with 0.5, 1, and 2% Er, respectively; whereas the temperature at which an obvious static recrystallization occurs increases with increasing Er, the temperature range being 315–335 °C for alloys with lower Er content and shifting to a higher temperature range of 350–365 °C for an increased Er content of 2%. The above results strongly supported the conclusion that when extruded at a lower temperature of 350 °C, Er promotes dynamic recrystallization during hot

deformation and helps a homogenous as-deformed microstructure, on the other hand, Er increases the critical static recrystallization temperature during the subsequent annealing treatment, or in other words, the Er-containing alloy has a higher tendency to resist static recrystallization.

3.2. As-annealed microstructures for alloys extruded at 420 °C

Increasing the extrusion temperature to 420 °C led to a complete DRX for all the alloys. The microstructural difference between alloys without and with Er addition is that an obvious abnormal grain growth has already occurred in the Er-free alloy; whereas the Er-bearing alloys display fine and uniform DRXed grains of 4–6 μm in size with no noticeable grain growth [18]. During subsequent annealing treatment, further grain growth occurred in all the experimental alloys and the alloys had different grain sizes when annealed at the same temperature. Figs. 5–7 show the as-annealed microstructures treated at different temperatures in the range of 250–400 °C for the 0, 0.5, and 4% Er-containing alloys extruded at 420 °C, respectively. The grain sizes at various annealing temperatures were measured for each alloy and the values are plotted in Fig. 8. These results reveal that the grain size increases with temperature and an abrupt growth occurs in the temperature range of 350–400 °C for all the alloys. Furthermore, with increasing Er content, the increase degree becomes weaker and the grain size decreases when annealed at the same temperature. The difference in size is certainly attributed to the different growth speed, which is in turn

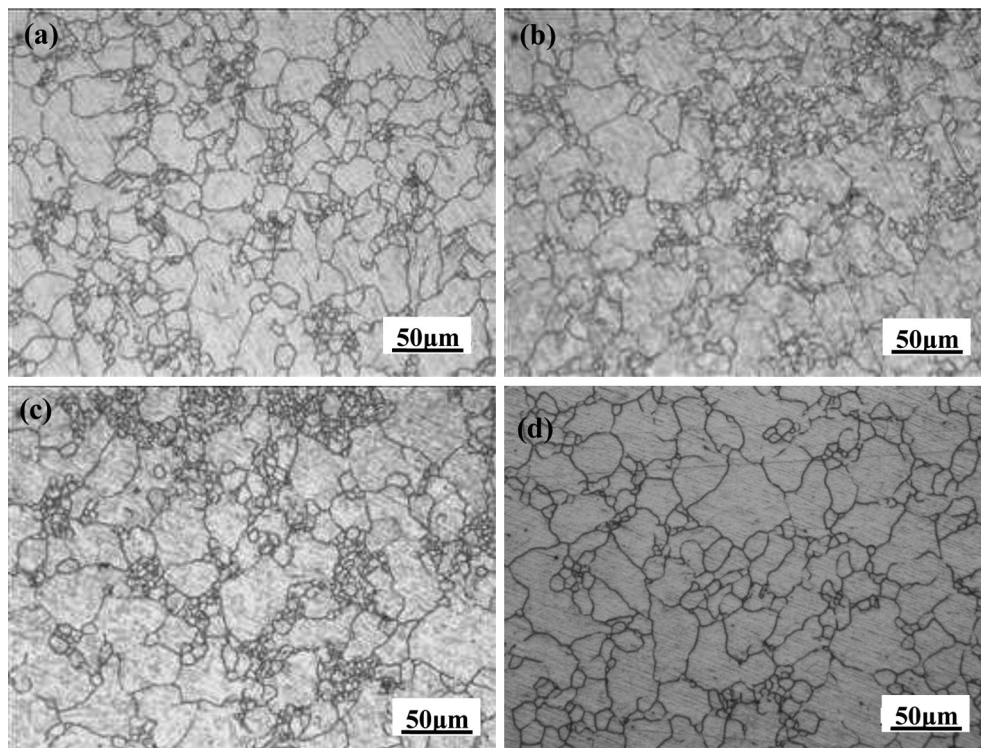


Fig. 5. Optical microstructures annealed at a) 250 °C, b) 300 °C, c) 350 °C, and d) 400 °C for Mg–1.5Zn–0.6Zr alloy extruded at 420 °C.

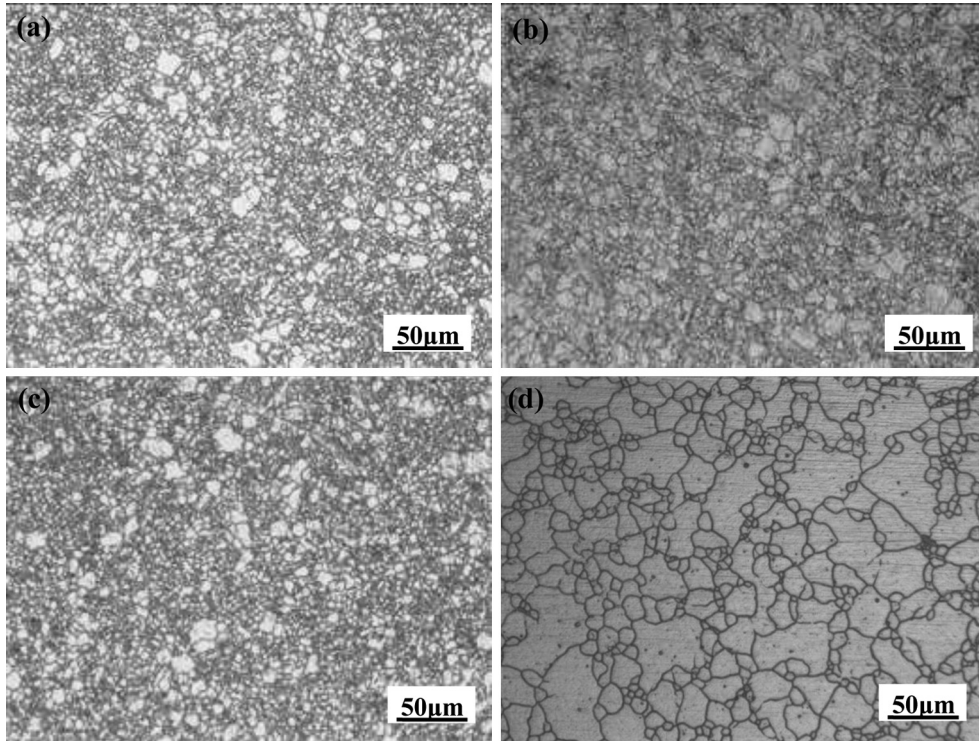


Fig. 6. Optical microstructures annealed at a) 250 °C, b) 300 °C, c) 350 °C, and d) 400 °C for Mg–1.5Zn–0.6Zr–0.5Er alloy extruded at 420 °C.

caused by different activation energy for grain boundary motion among alloys with different Er addition.

Grain growth is a thermal activation process. The average grain size \bar{D} at annealing temperature T holding for a period of time t follows equation:

$$\bar{D} - \bar{D}_0 = k \cdot t^m \exp(-Q/RT) \quad (1)$$

where \bar{D}_0 is starting grain size, k and m are materials constants, R is the universal gas constant, T is temperature in K, and Q the activation energy for grain boundary motion.

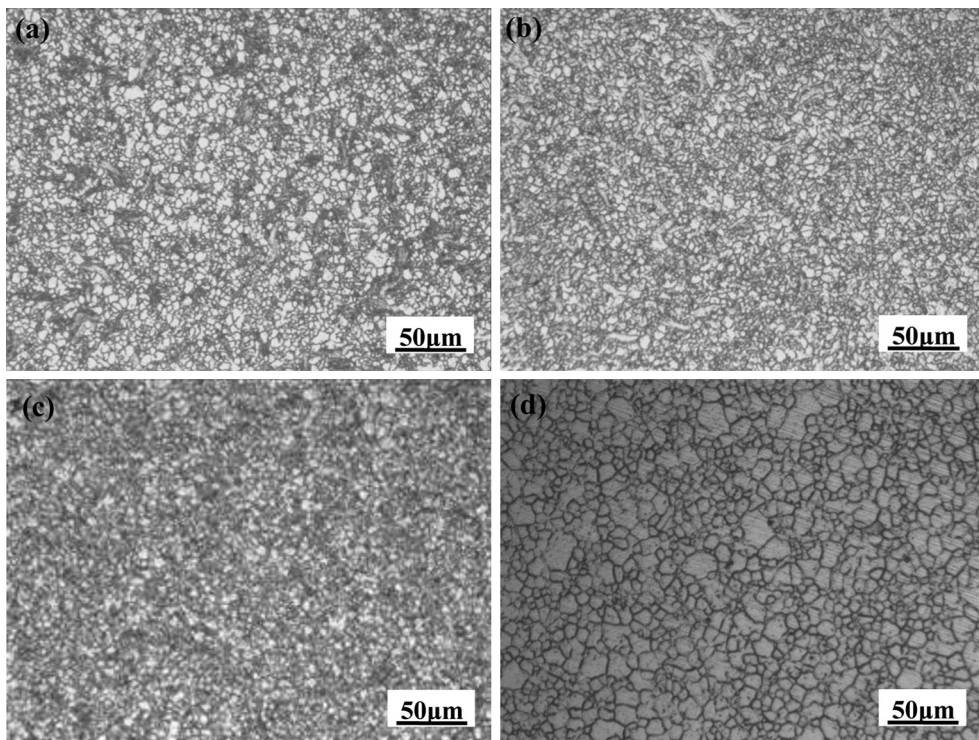


Fig. 7. Optical microstructures annealed at a) 250 °C, b) 300 °C, c) 350 °C, and d) 400 °C for Mg–1.5Zn–0.6Zr–4Er alloy extruded at 420 °C.

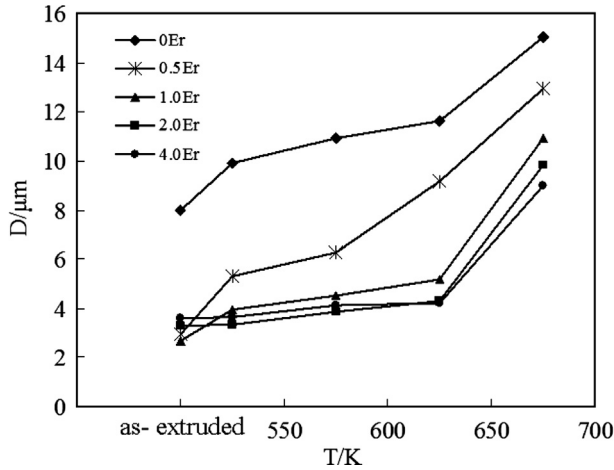


Fig. 8. Variation of grain size D with annealing temperature T for alloys with different Er addition.

The logarithm was taken and Eq. (1) was rearranged:

$$\lg \Delta D = \lg k + m \lg t - Q/RT \quad (2)$$

Substituting the experimental data into Eq. (2) yielded the $\lg \Delta D - 1/T$ plots for various Er-containing alloys, as given in Fig. 9. The slope of the $\lg \Delta D$ against $1/T$ plot then gave the value of Q/R . The calculated values of Q for each alloy are listed in Table 1.

The activation energy Q for Mg–1.5Zn–0.6Zr alloy is 23.8 kJ mol^{-1} . With the addition of Er, the activation energies increase. It is rather remarkable that the activation energy increases dramatically when the Er content reaches 2%, being 93.5 kJ mol^{-1} . Further increase of the Er content to 4% leads to a bit decline of the activation energy but still maintaining a fairly high value of Q , which is around 76 kJ mol^{-1} . The highest activation energy for grain boundary motion of the 2% Er-containing alloy implies that the alloy has the best thermal stability, which is well consistent with the microstructure observation results either extruded at $350 \text{ }^\circ\text{C}$ or $420 \text{ }^\circ\text{C}$.

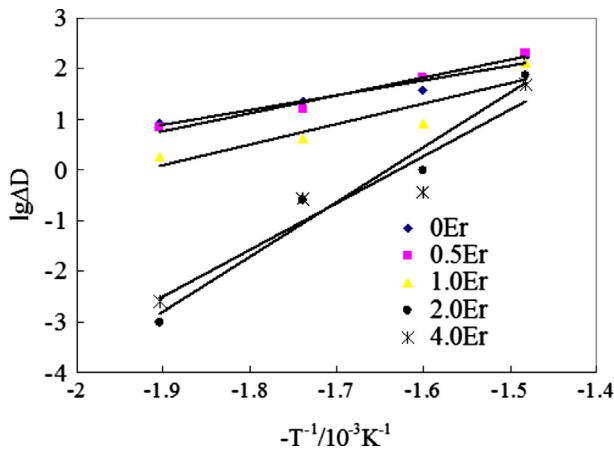


Fig. 9. The $\lg \Delta D$ against $1/T$ plots for various Er-containing alloys.

Table 1

Calculated values of Q for various Er-containing alloys.

Er contents (wt.%)	0	0.5	1.0	2.0	4.0
$Q \text{ (kJ mol}^{-1}\text{)}$	23.8	31.2	34.7	93.5	76.2

3.3. Discussion on the existing form and its effects of Er

From the above-mentioned results we can conclude that for the incomplete DRX microstructures extruded at a lower temperature of $350 \text{ }^\circ\text{C}$, Er addition increases the resistance of static recrystallization and for the complete DRX microstructures extruded at a relatively high temperature of $420 \text{ }^\circ\text{C}$, Er addition suppresses grain growth. The difference in microstructure stability is certain to relate to the microstructure feature. Previous studies [18,19] have shown that the addition of Er to Mg–1.5Zn–0.6Zr alloy results in the formation of a Mg–Zn–Er intermetallic phase, as well as a α -Mg solid solution dissolved more or less amount of Er. With the increase of Er addition, both the amount of the second-phase particles and the concentration of Er in α -Mg solid solution increase. Fig. 10 gives the variation of solute concentration of Er and second-phase-particle volume fraction with Er addition for Mg–1.5Zn–0.6Zr alloy. Both the intermetallic phase and the solute atoms of Er are believed to contribute to the thermal stability of the microstructure by grain boundary strengthening effect. Therefore, microstructure stability is improved with Er addition. It should be noted that although the 4% Er-containing alloy has the largest amount of the second-phase particles in its microstructure, as well as the highest Er concentration in the α -Mg solid solution, the activation energy for grain boundary motion is less than that of the alloy containing 2% Er. To clarify this point, we have to resort to more details of the existing forms of Er. Due to opposite lattice straining caused by Er and Zn solute atoms, it is expected that Er and Zn atoms in the solid solution tend to pair-up in neighboring sites to minimize the total energy caused by lattice distortion. Previous studies have confirmed the existence of such Er–Zn atom pairs and have revealed that the 2% Er-containing alloy

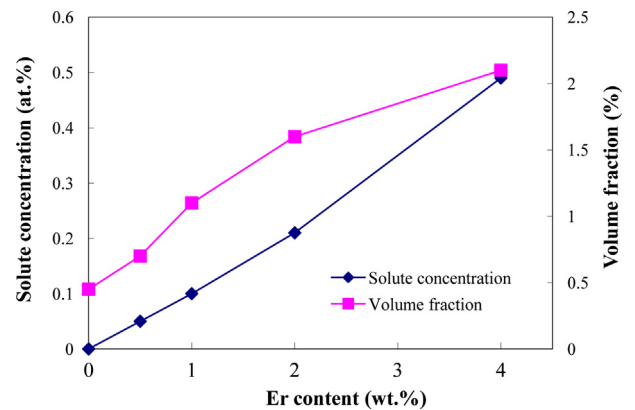


Fig. 10. Variation of solute concentration of Er and second-phase-particle volume fraction with Er addition for Mg–1.5Zn–0.6Zr alloy.

has the largest number of Er–Zn atom pairs [19]. The substantial increase in activation energy for the 2% Er-containing alloy may therefore be unambiguously attributed to the existence of a large number of Er–Zn atom pairs in α -Mg solid solution. It is then highly possible that it is the Zn–Er atom pair which favors the most to improve the thermal stability of the alloy.

4. Conclusions

Mg–1.5Zn–0.6Zr–0~4Er magnesium alloys were extruded at 350 °C and 420 °C to obtain microstructures with different dynamic recrystallization (DRX) degree and then undergone annealing treatment in the temperature range of 250–400 °C for a fixed time of 1.5 h. The effects of Er addition and its existing form on the static recrystallization and grain growth during annealing were studied. The results showed that for the incomplete DRX microstructures extruded at a lower temperature of 350 °C, the critical static recrystallization temperature increased with the increase of Er addition, the temperature range being 315–335 °C for alloys with lower Er addition and shifting to a higher temperature range of 350–365 °C for an increased Er content of 2%. Er addition increased the resistance of static recrystallization. For the complete DRX microstructures extruded at a relatively high temperature of 420 °C, Er addition suppressed grain growth. The activation energy for grain boundary motion for Er-free alloy was calculated to be 23.8 kJ mol⁻¹. A remarkable increase in activation energy was obtained in the 2% Er-containing alloy, being as high as 93.5 kJ mol⁻¹. The 2% Er-containing alloy manifested the best thermal stability. Both the intermetallic phase and the solute atoms of Er in α -Mg matrix contributed to the microstructure stability. Moreover, it is believed that the existing form of Er–Zn atom pairs in the α -Mg solid solution favored the most to improve the thermal stability of the alloy.

Acknowledgments

The authors are grateful for the financial support of the National Natural Science Foundation of China (No. 51271207) and sharing fund of Chongqing University's large-scale equipment.

References

- [1] J. Bohlen, P. Dobroň, J. Swiostek, D. Letzig, F. Chmelík, P. Lukác, K.U. Kainer, Mater. Sci. Eng. A 462 (2007) 302–306.
- [2] J. Koike, Metall. Mater. Trans. A 36A (2005) 1689–1696.
- [3] D.H. Sastry, Y.V.R.K. Prasad, K.I. Vasu, Scr. Mater. 3 (1969) 927–929.
- [4] D.H. StJohn, M. Qian, M.A. Easton, P. Cao, Z. Hildebrand, Metall. Mater. Trans. A 36A (2005) 1669–1679.
- [5] Y.B. He, Q.L. Pan, Y.J. Qin, X.Y. Liu, W.B. Li, J. Mater. Sci. 45 (2010) 1655–1662.
- [6] C.J. Bettles, M.A. Gibson, J. Met. 57 (2005) 46–49.
- [7] H. Takuda, S. Kikuchi, N. Hatta, J. Mater. Sci. 27 (1992) 937–940.
- [8] X.W. Zheng, J. Dong, Y.Z. Xiang, J.W. Chang, F.H. Wang, J. Li, et al., Mater. Des. 31 (2010) 1417–1422.
- [9] D.K. Xu, L. Liu, Y.B. Xu, E.H. Han, Mater. Sci. Eng. A 420 (2006) 322–332.
- [10] X.F. Guo, S. Remennik, C.J. Xu, D. Shechtman, Mater. Sci. Eng. A 473 (2008) 266–273.
- [11] J. Pelcová, B. Smola, I. Stuliková, Mater. Sci. Eng. A 462 (2007) 334–338.
- [12] W.B. Yu, Z.Y. Liu, H. He, N.P. Cheng, X. Li, Mater. Sci. Eng. A 478 (2008) 101–107.
- [13] S. He, L. Peng, X. Zeng, W. Ding, Y. Zhu, Mater. Sci. Eng. A 433 (2006) 175–181.
- [14] J. Bohlen, M.R. Nurnberg, J.W. Senn, D. Letzig, S.R. Agnew, Acta Mater. 55 (2007) 2101–2112.
- [15] Z.P. Luo, D.Y. Song, S.Q. Zhang, J. Alloys. Compd. 230 (1995) 109–114.
- [16] J. Zhang, Y.C. Dou, B.X. Zhang, X.D. Luo, Mater. Lett. 65 (2011) 944–947.
- [17] J. Zhang, M. Qi, F.S. Pan, Mater. Des. 31 (2010) 4043–4049.
- [18] J. Zhang, W.G. Li, B.X. Zhang, Y.C. Dou, Mater. Sci. Eng. A 528 (2011) 4740–4746.
- [19] J. Zhang, X.F. Zhang, W.G. Li, F.S. Pan, Z.X. Guo, Scr. Mater. 63 (2010) 367–370.